

Structure and properties degradation of the nuclear graphite under neutron irradiation

Boris A. Gurovich, Denis A. Kuleshov*, Dmitriy A. Maltsev, Oleg K. Chugunov, Alexey S. Frolov, Yaroslav I. Shtrombakh

National Research Center "Kurchatov Institute", 1, Akademika Kurchatova pl., Moscow, 123182, Russian Federation

*Corresponding author

DOI: 10.5185/amlett.2018.2132

www.vbripress.com/aml

Abstract

The operation of nuclear graphite in graphite-moderated reactors is accompanied by its properties degradation under the influence of neutron irradiation, which limits their service life. In this connection, it is of interest to identify the mechanisms that determine the properties degradation of graphite materials at various operational stages of operating RBMK power reactors. Copyright © 2018 VBRI Press.

Keywords: Nuclear graphite, neutron irradiation, power reactor, graphite, RBMK, electron microscopy, fractographic analysis, SEM, TEM.

Introduction

It is well known that operation of nuclear graphite in graphite-moderated reactors is accompanied by its properties degradation under neutron irradiation, which limits the lifetime of material. The features of radiation-induced changes of nuclear graphite properties in comparison with other structural materials used in nuclear reactors are due to the substantial anisotropy of graphite hexagonal crystal lattice and, accordingly, the properties of crystallites that form these materials. Moreover, the degree of properties macroscopic anisotropy of graphite-made products (for example, graphite blocks of nuclear reactor stacks) is determined by the texture that is due to the manufacturing technology.

It should be noted that almost complete lack of plasticity is typical for graphite. Most of nuclear-type graphites demonstrate quasi-brittle behavior[1–4], where failure occurs at very small strains (typical values are ~0.1-0.3% for tension, and 1-3% for compression[1, 5]). Stress cycling of graphite is characterized by hysteresis and residual strains (permanent set) that are attributed to these deformation processes[6]. Stress-strain curves for graphite demonstrate non-linear elastic deformation and rise of permanent set with increasing the load and number of loading cycles. Such nonlinear behavior is due to residual elastic strains (i.e. residual stress), which arise from the significant anisotropy of graphite crystals, that are expected in as-manufactured state of nuclear graphite[7–9] as was originally predicted by Mrozowski [10].

In this connection, the properties degradation of nuclear graphite as a result of irradiation (within the

framework of the present work) means a decrease in its mechanical characteristics (in particular, the elastic modulus and compressive strength) below the initial values.

The causes of nuclear graphite properties degradation under irradiation were previously discussed in[11–18]. In[13], the authors suggested that the properties degradation and cracking under irradiation of nuclear graphite samples (in the absence of macroscopic stresses) is caused by internal stresses that arise due to the difference in the radiation dimensional change rates of crystallites with different sizes. This assumption was associated with the features of the temperature dependence of crystallites radiation dimensional change rates obtained for highly oriented pyrolytic graphite (HOPG) with different final heat treatment temperatures (T_{fht}). However, the sizes of crystallites in HOPG with different T_{fht} were not previously determined by direct methods.

This paper continues the authors' work on the investigation of the mechanisms of degradation and destruction of nuclear graphite under neutron irradiation. In the present work high-resolution methods of scanning electron microscopy (SEM) were used: to study samples of HOPG with different T_{fht} ; to study the nature of destruction of nuclear graphite samples after mechanical tests (in the initial state and after various doses of irradiation); to study the character of destruction of graphite blocks. Such destruction is observed at the final stages of reactor operation, and it is important to determine the location of cracks in relation to the structural components (for example, with respect to boundaries of filler-binder type, filler-filler type, etc.).

Experimental

Materials

The following materials were studied in this paper:

1. HOPG specimens obtained by chemical vapor deposition process at 2100°C (as-deposited state) and the same specimens with subsequent heat treatment (under pressure of 10-30 MPa) at the following regimes: 2400, 2800°C and 3200°C for 3-5 h. All above-mentioned temperatures are T_{th} .
2. Trepanned graphite samples from graphite blocks of operating RBMK reactors (High power channel-type reactor).
3. Fragments of graphite blocks from operating RBMK power reactors, containing cracks formed during operation.

Methods

Elastic (Young's) modulus measurements by the dynamic method

Elastic modulus was measured by the dynamic method. Samples with diameter of 8-9 mm and length of 30-40 mm were used. These samples were made from nuclear graphite trepans cut by hollow mill of 10 mm diameter from graphite block stacks of RBMK type operating reactors in the direction perpendicular to the extrusion axis of the original graphite block.

The measurements were carried out in accordance with ASTM C747 standard in longitudinal vibration mode using the installation based on an audio frequency generator, piezo-radiators, amplifier and an oscilloscope. The installation scheme is given in the specified standard.

Ultimate strength determination under uniaxial compression

Ultimate strength were measured using uniaxial compression test of samples with diameter of 8-9 mm and length of 15-20 mm. These samples were made from nuclear graphite trepans cut by hollow mill of 10 mm diameter from graphite block stacks of RBMK type operating reactors in the direction perpendicular to the extrusion axis of the original graphite block.

The ultimate strength (compressive strength limit) was determined in accordance with ASTM C695 standard using the Hegewald & Peschke Inspect 50kN universal testing machine with 1 mm/min speed of the upper crosshead until specimen fracture (50% load drop of the maximum achieved value).

Transmission electron microscopy studies

TEM studies were carried out using FEI Titan 300 transmission electron microscope to reveal graphite structure degradation mechanisms under irradiation. TEM-specimen blanks in the form of disks with a 3 mm diameter and 0.5-1 mm thickness were manufactured using a precision saw Bervo Coring TCC and ultrasonic disc cutter Gatan Model 601. These disks were further

grinded on sandpaper (grain grade 1500) to achieve 120-150 μm thickness. Then the dimples with 1.5-2 mm diameter were formed on both sides using Dimpler D-500 installation, as a result a thin region of 20-40 μm thickness was formed in the specimen. After that the specimens passed two stages of ion milling using Gatan precision ion polishing system (PIPS) Model 691. At first stage an inclination angle of ion guns with respect to the specimen plane was 8°, and accelerating voltage was 5-5.5 kV, the thinning time varied from three to five hours depending on the specimen. In the second stage the corresponding angle was reduced to 6° and the accelerating voltage to 2 kV, the thinning time was 20-30 minutes.

Scanning electron microscopy studies

SEM studies were carried out using Carl Zeiss MERLIN scanning electron microscope:

- to determine the size of crystallites in HOPG;
- to study the fracture nature of trepanned graphite samples after uniaxial compression tests in the initial state and after neutron irradiation;
- to study the fracture nature of graphite blocks at the final stages of reactor operation.

To study the crystallite sizes in HOPG the sample surface was polished on a grinding paper with the following 3 minutes cleaning in an ultrasonic bath. The sample etching was carried out in a glow discharge at 1.1-1.4 kV voltage and 2-4 mA current for 8-20 minutes.

Analysis and discussion of structural studies results

TEM-studies results of graphite materials in initial state and after irradiation

The results of detailed TEM-studies of nuclear graphite in the initial and irradiated states were first presented in [13]. The studies both carried out in this paper (**Figs 1(a-c) and 2a**) and in [13] clearly demonstrated that GR-280 nuclear graphite that is widely used in RBMK reactors consists of several types of regions with a typical structure which is due to its manufacturing technology [19]. Primarily, there are of two region types with significant difference in crystallite average sizes in nuclear graphite corresponding to the filler (**Figs 1a and 1b**) and the binder (the left part of Fig. 1c). The size of the crystallites along the C axis in first region type (the filler) is ~ 40-100 nm and in the second type (the binder) – significantly smaller, ~ 3-10 nm. Both the filler and the binder regions consist of regions with different preferential orientation of the crystallites (basic planes) with lenticular (Mrozowski) cracks. The density and size of these cracks, as a rule, are the greater, the greater is the misorientation degree of the crystallites within the considered region (**Fig. 1**).

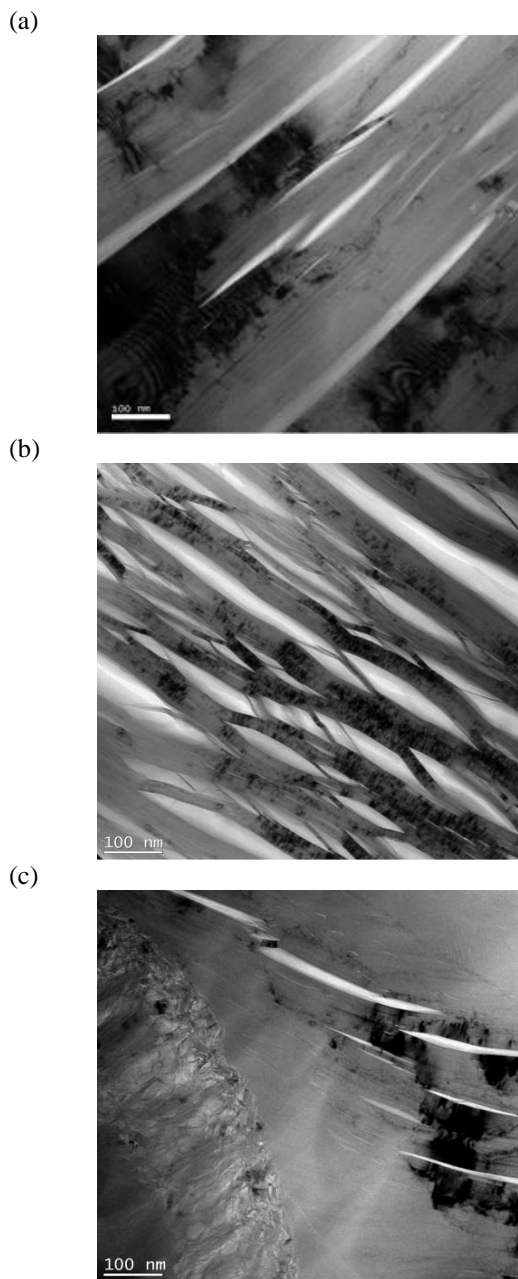


Fig. 1. Bright-field TEM-images of different region types in unirradiated nuclear graphite (a) filler region with a parallel or near-parallel crystallite packing, (b) filler region with deviation from a parallel crystallite packing, (c) filler-binder-filler boundary.

In addition, another kind of porosity due to the release of gaseous products arises during the technological processes of nuclear graphite manufacturing. As a result, the density of nuclear graphite at room temperature is 20-30 % lower than the theoretical one [20].

Fast neutron irradiation of nuclear graphite samples is accompanied by a significant change in their bulk density (up to 8-10 % volume change) [21]. These changes are due to several processes. The first one is the crystallite volume increasing due to the appearance of radiation defects and radiation dimensional change. The second one is reduction of the Mrozowski cracks

volume, which partially accommodate the radiation dimensional change. It leads, in many cases, to the appearance of shrinkage stage, followed by the so-called secondary swelling.

The studies in [13] showed that after irradiation of nuclear graphite at the temperature range of 400-600 °C up to neutron fluence corresponding to the maximum shrinkage, no significant structural changes except the partial closure of the oriented porosity were observed. After the beginning of the secondary swelling stage (i.e. at neutron fluence that correspond to the derivative sign change on the dose dependences of the volume changes), the fracture of the filler-binder boundaries begins to occur (**Fig. 2**). This effect was described in detail in [13]. Further, with the neutron fluence increase, the fracture of this boundaries type is more frequent.

It is important that such a fracture nature at the boundaries that separate the regions with close average crystallite sizes but with different preferential crystallite orientation (for example, “filler-filler” boundary type) are not observed in “two-phase” nuclear graphite at all the studied irradiation conditions. In this regard, it was first suggested in [13] that this fracture feature of “two-phase” nuclear graphite is due to the differences in the radiation dimensional change rates of crystallites with different sizes. At this, the localization regions of this fracture type are the filler-binder boundaries, where crystallites with different average sizes regularly coexist.

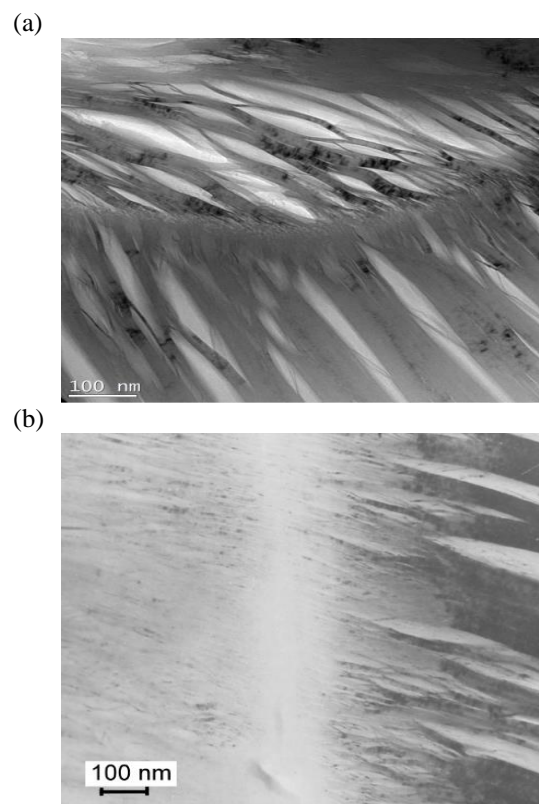


Fig. 2. Boundary types in nuclear graphite after neutron irradiation. (a) barely noticeable crystallite shredding on “filler-binder” type boundary, (b) initial stage of boundary destruction (“filler-binder” type boundary [13]).

Fractographic studies results of graphite materials

Along with the TEM-studies results of nuclear graphite samples, the results of fractographic studies after mechanical tests are also of great importance. Studies of the fracture nature of trepanned graphite samples are necessary to identify the structural mechanisms responsible for the cracking and subsequent fracture of nuclear graphite in graphite blocks both during irradiation at reactor operation and after mechanical tests at post-reactor research. In this paper trepanned samples from RBMK graphite blocks at different irradiation stages were investigated. Corresponding samples were subjected to a standard uniaxial compression test procedure, after which the fracture surface was examined by SEM.

Appearance of fractures of the “filler-binder” type boundaries under irradiation was observed in nuclear graphite samples irradiated without macroscopic stresses. The sources of such stresses under operation in nuclear reactor can be temperature and neutron fluence gradients in the volume and cross section of bulk graphite [22]. To confirm the significance of this mechanism during graphite operation as a part of core structural elements of nuclear reactor additional studies of trepanned samples from graphite-moderated reactor stacks are necessary. So in this paper the studies of graphite block fragments with cracks formed directly during the reactor operation were also investigated. This will confirm the universality of the structural factors that determine the mechanism and nature of graphite fracture both during reactor operation and at post-reactor tests.

A number of features are typical for nuclear graphite in comparison with the common structural materials (metals for example). In ordinary metallic polycrystalline materials a large-angle, small-angle and twin boundaries can be observed. Within the large-angle boundaries there are grains (crystallites) of the material, each of which has one crystal lattice orientation with the respect to arbitrarily chosen macroscopic axes. In the “two-phase” GR-280 nuclear graphite there are filler and binder areas since they are formed from different raw material types. These raw materials demonstrate dissimilar behavior during manufacture process resulting in different final structure and, as sequence, differences in the crystallite average sizes in filler and binder areas.

The boundaries between the filler and binder grains can be attributed to the large-angle boundaries by analogy with common materials.

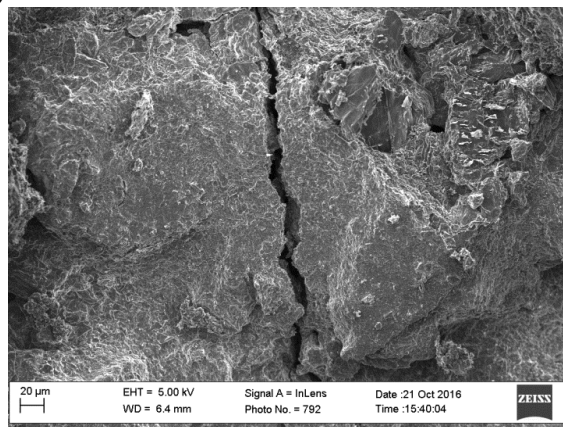
The boundaries of graphite materials in which the filler or/and binder grains coexist with each other (with different directions of preferential packing of the forming crystallites) can be classified (according to [13]), respectively, as “filler-filler”, “binder-binder” or “filler-binder” type boundaries. Destruction by any type of such boundaries here within the traditional approach can be regarded as intercrystalline and the “filler-binder” type boundary can be classified as “interphase” boundary in “two-phase” material.

At fractographic studies of structural materials (in particular metals and alloys) the relationship between the shares of fracture types (intercrystallite and transcrystallite) on the main crack surface after various mechanical tests or after its fracture during operation is usually used to identify the mechanisms responsible for fracture. At this, as the experience of fractographic studies shows, the structural mechanisms (types) of fracture that are observed on the primary main crack surface coincide with the fracture types typical for secondary cracks propagating approximately perpendicular to the primary fracture surface. For example, if the primary crack is formed solely by transcrystalline fracture (for example, by cleavage or quasi-cleavage), the secondary cracks will be also transcrystalline. If the primary fracture contains both transcrystalline and intercrystalline fracture regions, the secondary cracks on the main crack surface will also contain approximately the same ratio of intercrystalline and transcrystallite fracture sites. Thus, by the secondary cracks type it is possible to judge the fracture nature of the material at the main crack formation.

This consideration is relevant for the “two-phase” nuclear graphite, since the presence of the filler and binder grains, each of which includes a variety of crystallites, significantly complicates the analysis of the fracture nature using only the primary crack fracture structure. In this case, for an adequate classification of the fracture nature, it is necessary to take into account the fracture nature of the responding fracture part, which is practically impossible. Therefore, when determining the fracture type of “two-phase” nuclear graphite, the nature of the secondary cracks observed on the fracture surfaces (in the initial state and after neutron irradiation under various conditions) should be necessarily taken into account.

Fractographic studies of unirradiated GR-280 nuclear graphite after compression tests showed that the fracture surface is a set of regions with transcrystallite secondary cracks that correspond to the filler and/or binder regions (**Fig. 3a**). Herewith intercrystallite fracture along the “filler-binder” (or “filler-filler”) type boundaries is practically absent.

(a)



(b)

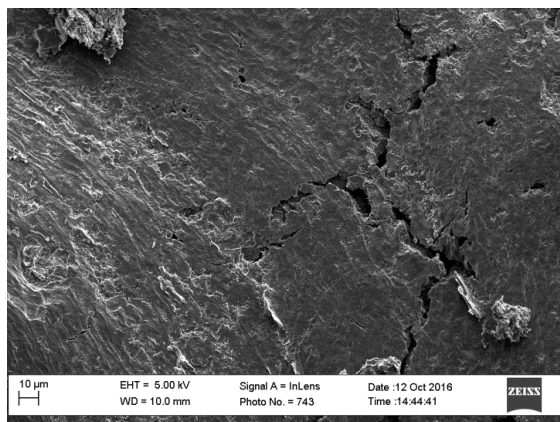
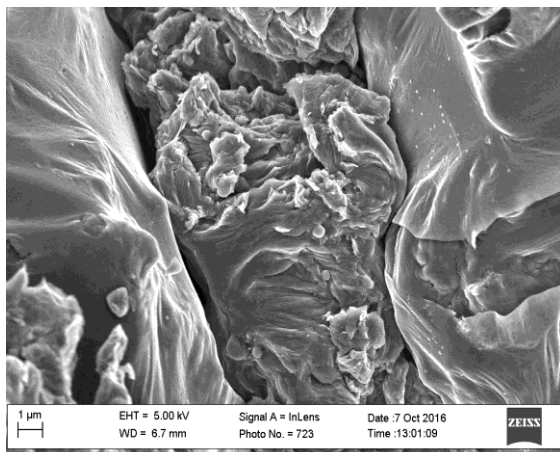


Fig. 3. Typical SEM-images of nuclear graphite fracture surface (a) secondary transcrystalline crack along the filler body in initial state, (b) secondary transcrystalline crack along the filler body after irradiation to a fluence close to the maximum shrinkage stage (turn-around dose).

Fractographic studies of GR-280 nuclear graphite trepanned samples after irradiation to fluence lower than position of the minimum on dose dependences of volume changes (turn-around dose, where the maximum volume shrinkage is observed) have shown that the nature of secondary cracks in comparison to the initial state does not change. The resulting secondary cracks are mainly transcrystalline (**Fig. 3b**) and the fracture on the “filler-binder” (or “filler-filler”) type boundaries are almost absent.

Fractographic studies of GR-280 nuclear graphite after irradiation up to neutron fluence above the turn-around dose (with a decrease in the mechanical properties to the values close to the initial one after primary radiation-induced increase) showed along with the presence of transcrystalline fracture, appearance of intercrystalline fracture regions along the “filler-binder” type boundaries (**Fig. 4a**). The further increase of neutron fluence, accompanied by degradation of all the main material properties, leads to the predominance of sites with fracture along the “filler-binder” type boundaries (**Fig. 4b**).

(a)



(b)

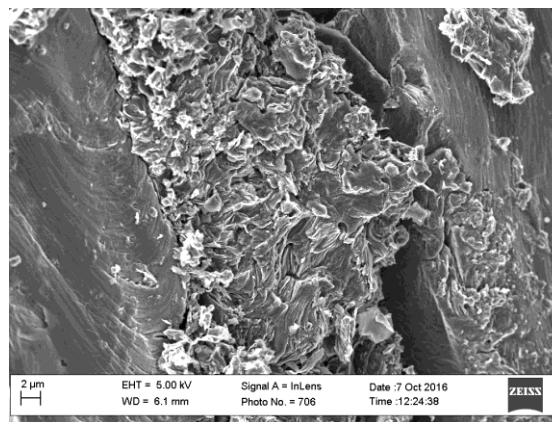
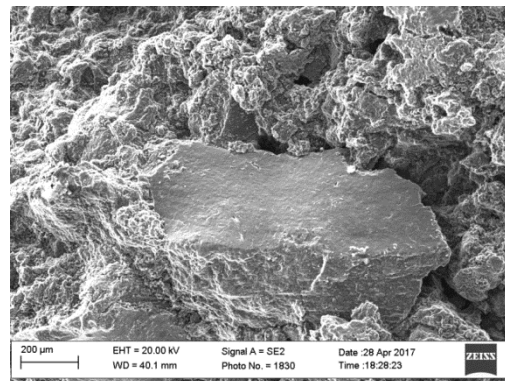


Fig. 4. Typical fracture surface of samples cut from nuclear graphite trepanns after compression test. (a), (b) secondary intercrystalline cracks in the filler-binder-filler region-Graphite were irradiated up to neutron fluence corresponding to the secondary swelling stage, where the rate of pore generation significantly exceeds the rate of pore closure.

This type of fracture is typical both for trepanned samples after compression post-reactor tests and for graphite blocks’ fragments containing fracture surfaces formed directly during operation (**Fig. 5**). Herewith the areas of fracture along the “filler-filler” and “binder-binder” boundary types are not observed.

(a)



(b)

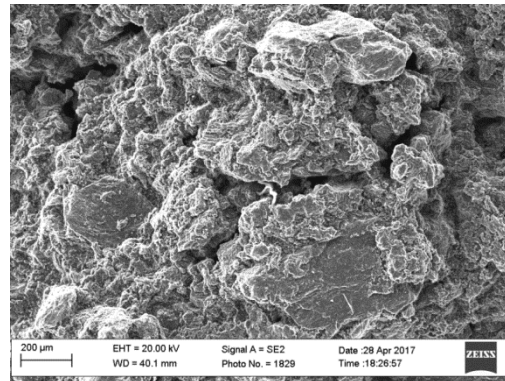


Fig. 5. Typical fracture surface of nuclear graphite blocks after irradiation (cracks occur during reactor operation). (a), (b) secondary intercrystalline cracks in the filler-binder area. Graphite were irradiated up to neutron fluence corresponding to the secondary swelling stage, where the rate of pore generation significantly exceeds the rate of pore closure.

Thus, the structural mechanism of nuclear graphite properties degradation irradiated both in the form of samples and as a part of graphite stack blocks is the same, and is determined by the fracture of the “filler-binder” type boundaries.

As mentioned above, it was suggested that the fracture of the “filler-binder” type boundaries is due to the difference in the rates of radiation dimensional change of the filler and binder crystallites. It was based on a well-known experimental fact about the influence of crystallite size on the rate of HOPG radiation dimensional change at elevated irradiation temperatures (see Fig. 6 [13]).

Fig. 6 shows that in the irradiation temperature range ~ 150-400 °C, the rate of radiation dimensional change does not depend on the crystallite size and decreases with irradiation temperature increase. With an increase of irradiation temperature from ~ 500 °C to ~ 900 °C, the radiation dimensional change rate increases and it is significantly larger for HOPG with smaller crystallite sizes. At this, the difference in the rates of radiation dimensional change increases with increasing irradiation temperature.

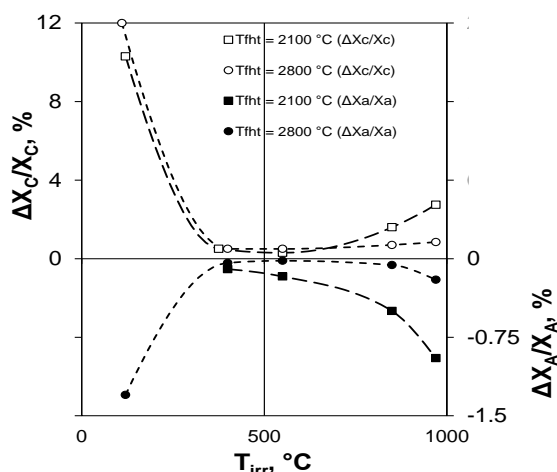


Fig. 6. Relative change in linear dimensions as a temperature function for HOPG samples with different treatment (graphitization) temperatures after neutron irradiation ($E > 0.18$ MeV) to fluence 4×10^{24} n/m² (replotted from [13]; lines are guide to the eye).

SEM-studies results of HOPG with different final heat treatment temperature

In this work study of HOPG in the initial state were carried out by high-resolution SEM methods (Fig. 7) to determine the influence of HOPG final heat treatment temperature on the size of the crystallites forming them. The results of measurements of the HOPG crystallite size are given in Table 1.

Table 1. The average crystallite sizes in HOPG with different T_{fht} .

| HOPG final heat treatment temperature, °C | Average crystallite size in C axis direction, nm |
|---|--|
| 2100 (as-deposited) | 5-7 (6±1) |
| 2400 | 10-20 (15±5) |
| 2800 | 20-30 (25±5) |
| 3200 | 40-50(45±5) |

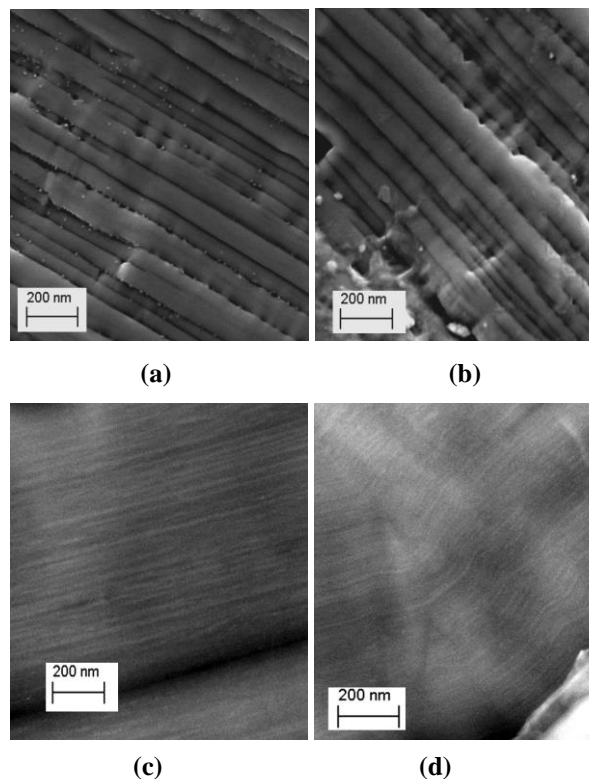


Fig. 7. Typical SEM images of crystallites in HOPG with different final heat treatment temperatures. (a) $T_{\text{fht}} = 3200$ °C, (b) $T_{\text{fht}} = 2800$ °C, (c) $T_{\text{fht}} = 2400$ °C, (d) $T_{\text{fht}} = 2100$ °C (as-deposited).

The data in Table 1 shows that the average crystallite sizes of HOPG with T_{fht} from 2100 °C to 3200 °C increase from 5-7 nm (at 2100 °C) to 40-50 nm (at 3200 °C) with the increase of T_{fht} . Herewith, the average HOPG crystallite size with the treatment temperature of 2100 °C is somewhat more or approximately equal to the average size of the binder crystallites in GR-280 graphite, and the average HOPG crystallite sizes with a treatment temperature of 2800-3200 °C are slightly smaller than the average filler crystallite sizes in GR-280 nuclear graphite. It should be noted that the HOPG crystallite size scatter is much less than the difference in the average sizes of the filler and binder crystallites. Moreover, in HOPG there are almost no regions, where crystallite pairs with a large difference in size systematically coexist.

Discussion

The obtained results confirm the validity of the transfer of the crystallite size effect on the rate of radiation dimensional change in HOPG to “two-phase” nuclear graphite for regions where crystallites regularly coincide with substantially different sizes (i.e., “filler-binder” type boundaries). This is a direct confirmation of the assumption made in [13]: the difference in the radiation dimensional change rate of the filler and binder crystallites cause the appearance and growth of internal stresses at the filler-binder boundaries during irradiation.

Ultimately, these stresses lead to the crack formation on the “filler-binder” type boundaries and, as a result, to the properties degradation of nuclear graphite samples even in the absence of external stresses.

An important additional confirmation of the proposed properties degradation model of nuclear graphite under irradiation is the difference in dose dependences of volume changes and elastic modulus changes of GR-280 and MPG-6 graphites. **Fig. 8** [13] presents the dose dependence of the volume change and elastic modulus of “two-phase” GR-280 nuclear grade graphite and MPG-6 industrial grade graphite after irradiation under the same conditions. MPG-6 is manufactured based on uncalcined petroleum coke as the filler. These cokes usage facilitates the formation of a monolithic structure without distinct boundaries between the coke-filler and coke-binder areas, thus affecting the dimensional stability of a products made from such graphite [23, 24]. MPG-6 has almost no noticeable difference in structure between the binder and filler regions, and also has smaller crystallite size dispersion [25]. Such graphites can be called “single-phase” in contrary to conventional “two-phase” GR-280 graphite.

Fig. 8 shows that a derivative sign change on the dose dependence of elastic modulus for GR-280 graphite is observed upon reaching a neutron fluence of about 2×10^{25} n/m² at irradiation temperature of 900-1000 °C. At higher neutron fluence there is a pronounced decrease in mechanical properties with irradiation dose increase [25]. Comparison of the dose dependence of the elastic modulus change for GR-280 graphite at irradiation temperatures of 500-600 °C and 900-1000 °C shows that in the second case neutron fluence at which the derivative sign changes is approximately three times lower. This effect is due to the higher influence of the difference between the filler and binder crystallite size on the rate of radiation dimensional change at higher irradiation temperature (Fig. 6) and, as a consequence, the degradation rate is much higher.

For GR-280 graphite, where the filler and binder crystallite sizes differ significantly, a typical dose dependence of the elastic modulus change is observed as a result of irradiation in the temperature range 300-800 °C (with a change of derivative sign and the appearance of the region where the absolute values of elastic modulus begin to drop noticeably to the close to the original value, see Fig. 8). For MPG-6 graphite with the close filler and binder crystallite sizes irradiation under the same conditions does not lead to the change of derivative sign on the dose dependences of elastic modulus, its absolute value grows monotonically (see Fig. 8). It is significant that this behavior of the “single-phase” MPG-6 graphite under irradiation is observed at much larger (approximately 3 times) volume changes (see Fig. 8). This indicates that in general case the magnitude and sign of graphite volume changes itself as

a result of irradiation cannot be a criterion of the properties degradation degree of nuclear graphite.

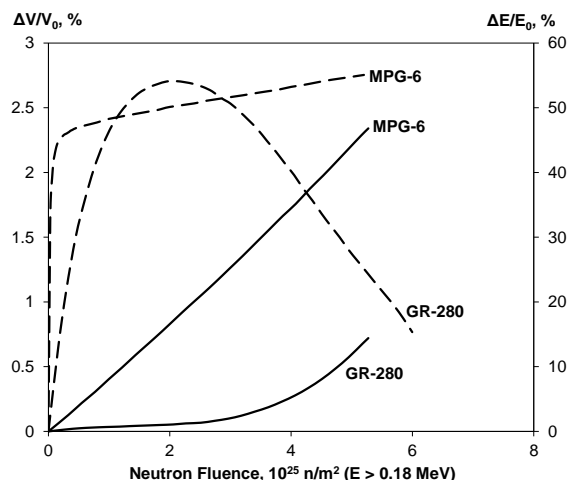


Fig. 8. Dose dependences of the volume changes (solid lines) and elastic modulus (dashed lines) of “single-phase” MPG-6 and “two-phase” GR-280 graphite irradiated under the same conditions at the temperature 900-1000 °C (replotted from [13]).

Conclusions

Neutron irradiation of nuclear graphite samples leads to internal stresses due to the presence of significant misorientation of crystallographic C axes in grains (areas) with different preferential crystallite packing. However, at low irradiation temperatures (~150-400 °C), significant radiation-induced volume changes in graphite do not lead to its mechanical properties degradation. At temperatures above ~500-600 °C, irradiation is accompanied by the properties degradation, that occurs when a certain neutron fluence is reached, which is the smaller the higher the irradiation temperature.

Fractographic studies of trepanned samples from graphite blocks of operating RBMK-type reactors showed the following. In initial state and after irradiation to fluence smaller than the turn-around dose, the fracture of graphite is “transcrystallite”, that is, through regions that are not “filler-filler”, “binder-binder” and “filler-binder” boundaries. Upon irradiation to neutrons above the turn-around dose, the fracture along the “filler-binder” type boundaries begin to appear, and then, to dominate with increasing neutron fluence. This confirms the argument made in [13] for the first time that the boundaries of regions with different crystallite average sizes (i.e., the “filler-binder” type boundaries) and its fracture due to the difference in the rates of radiation dimensional change are the main mechanism determining the observed properties degradation of “two-phase” nuclear graphite. These effects are all the more significant the higher the irradiation temperature in the temperature range, where the crystallite sizes affect the radiation dimensional change rate.

Acknowledgements

The authors express their gratitude to Dr. E.A. Kuleshova for significant contribution in preparing of this article, Dr. S.V. Fedotova for editing and translating of the original text, Dr. A.D. Erak for editing and translating of the original text and great assistance in preparation and edition of this article.

References

1. R. Taylor, R.G. Brown, K. Gilchrist, E. Hall, A.T. Hodds, B.T. Kelly, and F. Morris: "The mechanical properties of reactor graphite." *Carbon N. Y.* vol. 5, no. 5, pp. 519–531, 1967.
2. T.J. Marrow, D. Liu, S.M. Barhli, L. Saucedo Mora, Y. Vertyagina, D.M. Collins, C. Reinhard, S. Kabra, P.E.J. Flewitt, and D.J. Smith: "In situ measurement of the strains within a mechanically loaded polygranular graphite." *Carbon N. Y.* vol. 96, no. September, pp. 285–302, 2016.
3. D. Liu, P.J. Heard, S. Nakhodchi, and P.E.J. Flewitt: "Small-Scale Approaches to Evaluate the Mechanical Properties of Quasi-Brittle Reactor Core Graphite." Graphite Testing for Nuclear Applications: The Significance of Test Specimen Volume and Geometry and the Statistical Significance of Test Specimen Population. pp. 84–104. *ASTM International*, 100 Barr Harbor Drive, PO Box C700, West Conshohocken, PA 19428-2959 (2014).
4. D. Liu, K. Mingard, O.T. Lord, and P. Flewitt: "On the damage and fracture of nuclear graphite at multiple length-scales." *J. Nucl. Mater.* vol. 493, pp. 246–254, 2017.
5. W.N. Reynolds: "The mechanical properties of reactor graphite." *Philos. Mag.* vol. 11, no. 110, pp. 357–368, 1965.
6. G.B. Neighbour and B. McEnaney: "Creep and recovery in graphites at ambient temperature: An acoustic emission study." *Carbon N. Y.* vol. 32, no. 4, pp. 553–558, 1994.
7. L. Delannay, P. Yan, J.F.B. Payne, and N. Tzelepi: "Predictions of inter-granular cracking and dimensional changes of irradiated polycrystalline graphite under plane strain." *Comput. Mater. Sci.* vol. 87, pp. 129–137, 2014.
8. B. Rand: "Towards a Structural Basis to the Physical Properties of Irradiated Polycrystalline Nuclear Graphite." Modelling and Measuring Reactor Core Graphite Properties and Performance. pp. 2–8. *Royal Society of Chemistry*, Cambridge, U.K (2012).
9. M. Kuroda, S.L. Fok, B.J. Marsden, and S.O. Oyadiji: "Dynamics and generation of stress waves in cracked graphite moderator bricks." *Nucl. Eng. Des.* vol. 235, no. 5, pp. 557–573, 2005.
10. S. Mrozowski: "Mechanical strength, thermal expansion and structure of cokes and carbons." *Proc. First Second Conf. Carbon Held Buffalo, New York, 1953 1955.* pp. 31–45, 1956.
11. T.D. Burchell and L.L. Snead: "The effect of neutron irradiation damage on the properties of grade NBG-10 graphite." *J. Nucl. Mater.* vol. 371, no. 1–3, pp. 18–27, 2007.
12. P. a. Platonov, I.F. Novobratskaya, Y.P. Tumanov, V.I. Karpukhin, and S.I. Alekseyev: "Effect of neutron irradiation on the dimensional stability of graphite pre-treated at different temperatures." *Radiat. Eff.* vol. 54, no. 1–2, pp. 91–97, 1981.
13. Y.I. Shtrombakh, B.A. Gurovich, P.A. Platonov, and V.M. Alekseev: "Radiation damage of graphite and carbon-graphite materials." *J. Nucl. Mater.* vol. 225, pp. 273–301, 1995.
14. D.E. Baker: "Graphite as a neutron moderator and reflector material." *Nucl. Eng. Des.* vol. 14, no. 3, pp. 413–444, 1971.
15. B.T. Kelly: "Graphite – the most fascinating nuclear material." *Carbon N. Y.* vol. 20, no. 1, pp. 3–11, 1982.
16. J.H. Cox and J.W. Helm: "Graphite irradiations 300°–1200°C." *Carbon N. Y.* vol. 7, no. 2, pp. 319–327, 1969.
17. I.G. Lebedev and Y.S. Virgil'ev: "Comparative tests of the radiation resistance of reactor graphite." *At. Energy.* vol. 85, no. 5, pp. 796–801, 1998.
18. I.G. Lebedev, O.G. Kochkarev, and Y.S. Virgil'ev: "Radiation-induced change in the properties of isotropic structural graphite." *At. Energy.* vol. 93, no. 1, pp. 589–594, 2002.
19. T.D. Burchell: "Radiation effects in graphite." *Comprehensive Nuclear Materials.* pp. 299–324. *Elsevier Inc.* (2012).
20. V.N. Barabanov and Y.S. Virgil'ev: "Radiacionnâ pročnost' konstrukcionnogo grafita [Radiation strength of structural graphite] [In Russian]." *Atomizdat*, Moscow, 1976.
21. S. V. Šulepov: "Fizika uglegrafitovykh materialov [Physics of carbon-graphite materials] [In Russian]." *Metallurgîa [Metallurgy]*, Moscow, 1972.
22. D.K.L. Tsang and B.J. Marsden: "The development of a stress analysis code for nuclear graphite components in gas-cooled reactors." *J. Nucl. Mater.* vol. 350, no. 3, pp. 208–220, 2006.
23. G.B. Engle: "Properties and high-temperature irradiation behavior of graphites prepared with uncalcined coke." *Carbon N. Y.* vol. 6, no. 4, pp. 447–454, 1968.
24. I.P. Kalyagina and Y.S. Virgil'ev: "Radiation dimensional stability of graphite with an uncalcined coke-filler." *Sov. At. Energy.* vol. 55, no. 3, pp. 588–591, 1983.
25. Y.I. Shtrombakh, P.A. Platonov, B.A. Gurovich, and V.M. Alekseev: "Radiation behaviour of graphite for HTGR." *International Atomic Energy Agency (IAEA)*, 1996.